23. Z. A. Peterlin, J. Kozloski, B. Q. Mao, A. Tsiola, R. Yuste, *Proc. Natl. Acad. Sci. U.S.A.* **97**, 3619 (2000).
24. M. Bazhenov, I. Timofeev, M. Steriade, T. J. Sejnowski, *J. Neurosci.* **22**, 8691 (2002).
25. R. S. Zucker, W. Regehr, *Annu. Rev. Physiol.* **64**, 355 (2002).
26. G. Silberberg, H. Markram, *Neuron* **53**, 735 (2007).
27. D. A. McCormick, T. Bal, *Annu. Rev. Neurosci.* **20**, 185 (1997).
28. E. F. Pace-Schott, J. A. Hobson, *Nat. Rev. Neurosci.* **3**, 591 (2002).
29. B. E. Jones, *Prog. Brain Res.* **145**, 157 (2004).
30. This work was supported by grants from NIH and NSF (SBE-0542013 to Temporal Dynamics of Learning Center, TDLC). We thank W. Sun for technical help.

Supporting Online Material
www.sciencemag.org/cgi/content/full/324/5927/643/DC1
Materials and Methods
Figs. S1 and S2

18 December 2008; accepted 13 March 2009
10.1126/science.1169957

Self-Control in Decision-Making Involves Modulation of the vmPFC Valuation System

Todd A. Hare,[1]* Colin F. Camerer,[1,2] Antonio Rangel[1,2]

Every day, individuals make dozens of choices between an alternative with higher overall value and a more tempting but ultimately inferior option. Optimal decision-making requires self-control. We propose two hypotheses about the neurobiology of self-control: (i) Goal-directed decisions have their basis in a common value signal encoded in ventromedial prefrontal cortex (vmPFC), and (ii) exercising self-control involves the modulation of this value signal by dorsolateral prefrontal cortex (DLPFC). We used functional magnetic resonance imaging to monitor brain activity while dieters engaged in real decisions about food consumption. Activity in vmPFC was correlated with goal values regardless of the amount of self-control. It incorporated both taste and health in self-controllers but only taste in non–self-controllers. Activity in DLPFC increased when subjects exercised self-control and correlated with activity in vmPFC.

The concept of self-control in decision-making has occupied philosophers and scientists throughout recorded history because the ability to exercise it is central to human success and well-being. Behavioral studies have examined the problem of self-control and provided valuable insights that suggest it is exhaustible in the short term (*1*–*3*), can be enhanced by cognitive strategies (*4*–*7*), and is correlated with measures of intelligence (*8*–*10*). However, little is known about the neurobiological underpinnings of self-control and how these neural mechanisms might differ between successful and unsuccessful self-controllers.

We investigated which neural processes are responsible for the deployment of self-control and how these processes interact with the brain's valuation and decision-making circuitry. We hypothesized that goal-directed decisions have their basis in a value signal encoded in the ventromedial prefrontal cortex (vmPFC). This hypothesis has its basis in neuroimaging studies that have found a correlation between activity in this area and behavioral measures of value (*11*–*16*), as well as findings from electrophysiology studies (*17*, *18*). We also hypothesized that self-control involves modulation by the dorsolateral prefrontal cortex (DLPFC) of the value signals computed in vmPFC. This hypothesis has its basis in the role of DLPFC in cognitive control (*19*, *20*), working memory (*21*, *22*), and emotion regulation (*23*).

To test these hypotheses, we recruited self-reported dieters and used functional magnetic resonance imaging (fMRI) to study the neural activity in vmPFC and DLPFC while the participants made real decisions about which foods to eat. Participants performed three tasks in the scanner (Fig. 1A) (*24*). In the first two parts, they rated 50 different food items for taste and health separately. On the basis of these ratings, we selected a reference item for each subject that was rated neutral in both taste and health. In the final part, subjects were asked to choose between each of the foods and the reference item. One decision was randomly selected and implemented at the end of the study. Participants indicated the strength of their decision by using a five-point scale (strong no, no, neutral, yes, and strong yes), which provided a measure of their relative value for eating that food instead of the reference item. Following the previous literature (*11*), we refer to this measure as a goal value, which refers to the amount of expected reward associated with consuming the food. Note that dieters should be concerned with the healthiness of the foods, and not only with their taste, and that optimal decision-making requires integrating these two separate concerns.

Participants were classified as self-controllers (SCs; $n = 19$) or non–self-controllers (NSCs; $n = 18$) on the basis of their decisions (*24*). There was a stark difference between the SC and NSC groups (Fig. 1B): Whereas SCs made decisions on the basis of both health and taste, rejecting most liked-but-unhealthy items, the NSC group made decisions on the basis of taste alone.

We made four predictions about the patterns of neural activity, which we tested by using the fMRI data. First, activity in vmPFC should be correlated with participants' goal values regardless of whether or not they exercise self-control. Second, activity in the vmPFC should reflect the health ratings in the SC group but not in the NSC group. Third, the DLPFC should be more active during successful than failed self-control trials. Fourth, DLPFC and vmPFC should exhibit functional connectivity during self-control trials.

We tested the first prediction by estimating a general linear model (GLM) of blood oxygen

[1]Division of Humanities and Social Sciences, California Institute of Technology, Pasadena, CA 91125, USA. [2]Computational and Neural Systems, California Institute of Technology, Pasadena, CA 91125, USA.

*To whom correspondence should be addressed. E-mail: thare@hss.caltech.edu

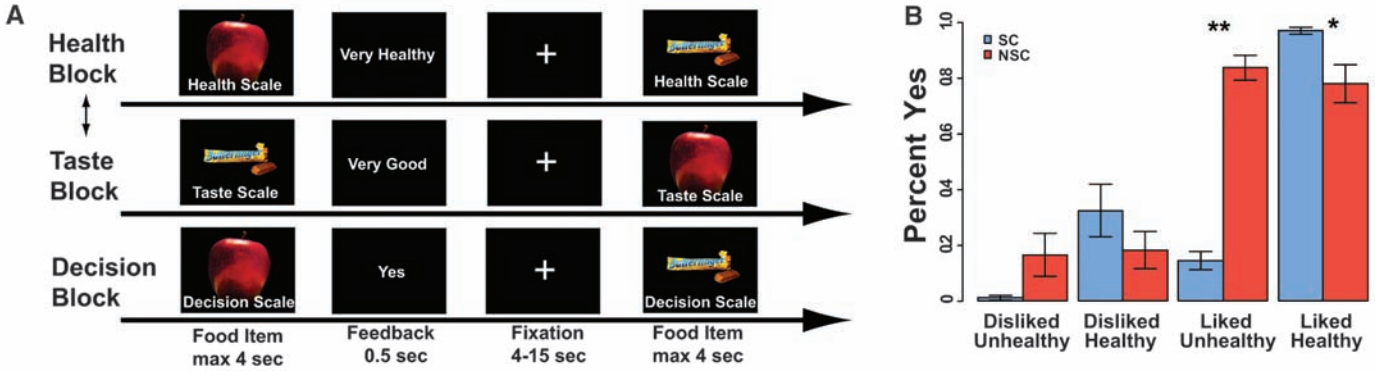

Fig. 1. (**A**) The task proceeded in three parts: taste ratings, health ratings, and decisions. (**B**) Percentage of the time participants chose the food over the reference item. The SC group chose not to eat liked-unhealthy food items more often than the NSC group did (**$t_{31} = 12.5$; $P < 0.0000$). The SC group also ate liked-healthy food items more often than the NSC group did (*$t_{18} = 2.74$; $P < 0.05$). Error bars denote standard errors.

level–dependent activity that included a parametric regressor for goal values at the time of evaluation. Activity in vmPFC was correlated with goal values for all participants regardless of the amount of self-control exercised (Fig. 2, A and B; fig. S1; and table S2). The areas of vmPFC identified largely overlap with regions that have been associated with valuation in other tasks that require no self-control (*11*–*15*) (Fig. 2C).

To test the second prediction, we estimated a new GLM that included parametric regressors for health and taste ratings. The beta values for both parametric regressors were extracted from the voxels in vmPFC that exhibited the strongest correlation with goal values for each participant. In the SC group, vmPFC activity was modulated by both health ($t_{18} = 4.20$, $P < 0.001$) and taste ($t_{18} = 3.31$, $P < 0.005$) (Fig. 2D), whereas in the NSC group it was only modulated by taste ($t_{17} = 7.28$, $P < 0.001$). We tested this relationship further by estimating a linear regression of the impact of health ratings on each participant's behavior against a measure of the impact of health ratings on the participant's vmPFC activity (regression coefficient = 0.847, $t_{35} = 5.57$, $P < 0.001$) (Fig. 2E).

We tested the third prediction by comparing the neural responses during the decision period in three different types of trials: those in which self-control was not needed, those in which self-control was successfully deployed, and those in which participants failed to use self-control. We found greater left DLPFC activity [inferior frontal gyrus (IFG) and Brodmann's area (BA) 9 (IGF/BA9)] in the SC group than in the NSC group during successful self-control trials (Fig. 3A and table S3). However, both groups had greater activity in this region for successful self-control trials compared with that of failed self-control trials (SC group $t_{14} = 2.29$, NSC group $t_{13} = 2.62$, $P < 0.05$) (Fig. 3B).

We tested the fourth prediction by performing a linear regression of left DLPFC activity during self-control trials on the response of vmPFC to the presentation of liked-but-unhealthy food items (regression coefficient = –0.688, $t_{17} = –2.26$; $P < 0.05$) (Fig. 3C). Self-control in this type of trial requires ramping down the weight given to taste in computing the goal value. A similar decrease in vmPFC activity was seen in gamblers who chose not to gamble in losing conditions (*25*).

We also investigated whether left DLPFC and vmPFC exhibited task-related functional connectivity. An initial analysis of the psychophysiological interactions (PPI) using left DLPFC as the seed showed connectivity with several regions (fig. S4 and table S4), including the left IFG/BA46 but not the vmPFC, which ruled out direct modulation from DLPFC. However, DLPFC might modulate the vmPFC through its effect in a third region, such as IFG/BA46. This area was of particular interest because it is involved in working memory and goal maintenance (*21*, *22*), it has anatomical connections to vmPFC (*26*), and previous studies have shown that IFG/BA46 activity is correlated with goal values (*11*, *13*). Thus, we used this area as the seed for a second PPI analysis and found positive task-related functional connectivity with the vmPFC (fig. S3 and table S5). A conjunction analysis confirmed that this was the same area of vmPFC that was correlated with goal values. Thus, the vmPFC was functionally connected to the left DLPFC through a two-node network (Fig. 4, B and C).

The results provide insight into two open questions in behavioral neuroscience. First, they suggest that self-control problems arise in situations where various factors (e.g., health and taste) must be integrated in vmPFC to compute goal values and that DLPFC activity is required for higher-order factors, such as health, to be incorporated into the vmPFC value signal. We speculate that the vmPFC originally evolved to forecast the short-term value of stimuli and that humans developed the ability to incorporate long-term considerations into values by giving structures such as the DLPFC the ability to modulate the basic value signal.

Second, a fundamental difference between successful and failed self-control might be the extent to which the DLPFC can modulate the vmPFC. Individual differences in the ability of DLPFC to modulate vmPFC might be due to differences within the DLPFC or to differences in connectivity between the DLPFC and other areas. The areas of DLPFC that we have found to play a role in self-control are similar to areas that are at work in cognitive control (*27*, *28*) and in emotional regulation (*23*, *29*). Our results are consistent with previous theories of the role of DLPFC in cognitive control, which posit that it sends signals to other brain regions to promote task-relevant processing and suppress irrelevant activity (*20*). Thus, our findings could be the start of an explanation for why general intelligence, cognitive control, and emotional regulation are all correlated with various behavioral measures of self-control (*5*, *8*–*10*).

Our findings also have implications for an ongoing debate in decision neuroscience and psychology. McClure *et al*. (*30*, *31*) have proposed that intertemporal choice involves the interaction of multiple independent valuation systems (some characterized by very large discount rates and a hypersensitivity to immediate rewards and others that are more patient and thus more sensitive to long-term considerations) that compete with each other for behavioral control. They have also proposed that the shortsighted valuation network includes the vmPFC and that the foresighted one includes the DLPFC. In contrast, Kable and Glimcher (*12*) have argued that there is a common valuation system and that the values that guide behavior are computed in the vmPFC-striatal network. However, they do not provide any theory or evidence about which neural mechanisms

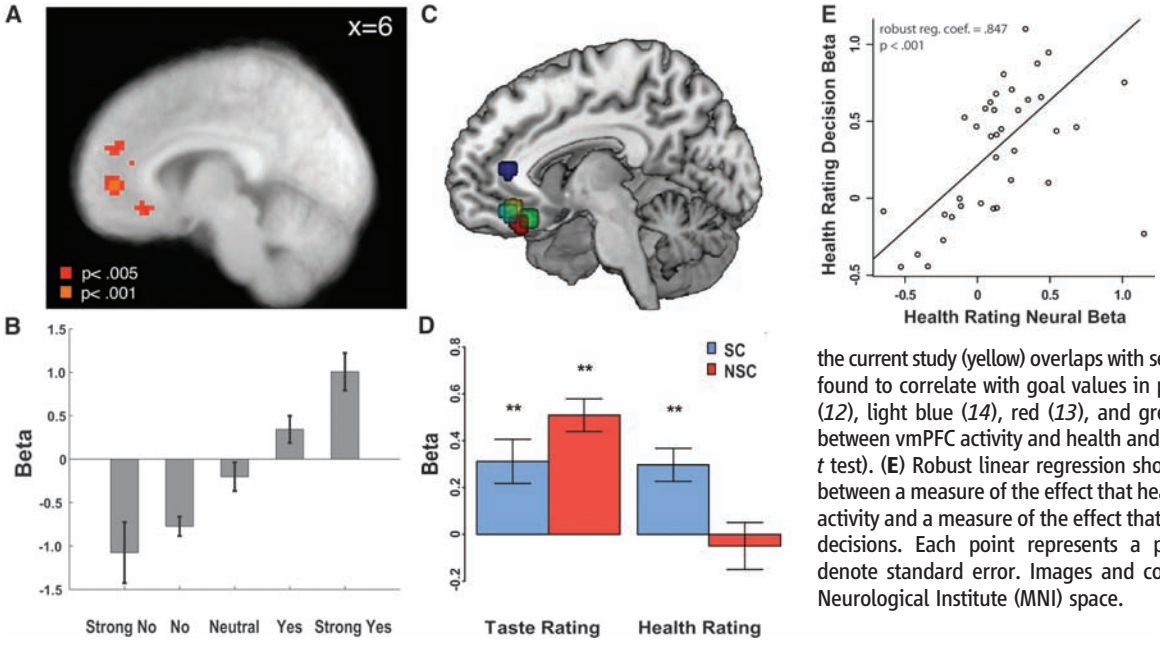

Fig. 2. (**A**) Regions of vmPFC in which activity correlated with goal values across all participants and regardless of their degree of self-control. See tables S1 to S5 for the statistics corrected for multiple comparisons. (**B**) Beta values in vmPFC increased with goal values. (**C**) The vmPFC area reflecting goal values in the current study (yellow) overlaps with several areas that have been found to correlate with goal values in previous studies [dark blue (*12*), light blue (*14*), red (*13*), and green (*11*)]. (**D**) Correlations between vmPFC activity and health and taste ratings (**$P < 0.005$, *t* test). (**E**) Robust linear regression showing a strong relationship between a measure of the effect that health ratings have on vmPFC activity and a measure of the effect that the health ratings have on decisions. Each point represents a participant. All error bars denote standard error. Images and coordinates are in Montreal Neurological Institute (MNI) space.

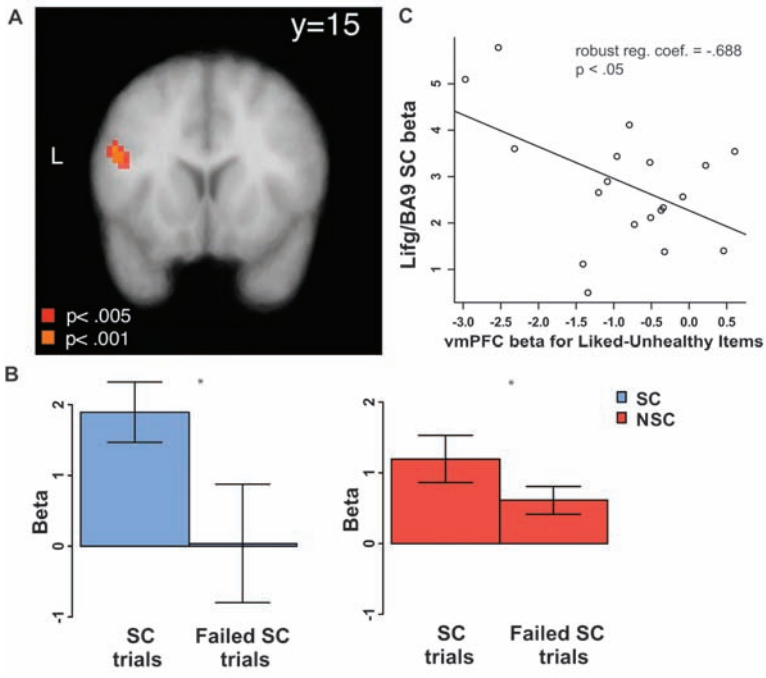

Fig. 3. (**A**) Region of left DLPFC showing greater activity in successful self-control trials in the SC than the NSC group. Images and coordinates are in MNI space. (**B**) Both groups showed greater activity in DLPFC for successful versus failed self-control trials (*$P < 0.05$, paired t test). (**C**) Activity in left DLPFC (IFG/BA9) was negatively correlated with vmPFC activity in the SC group during trials in which liked-but-unhealthy foods were avoided. Each point represents a participant in the SC group.

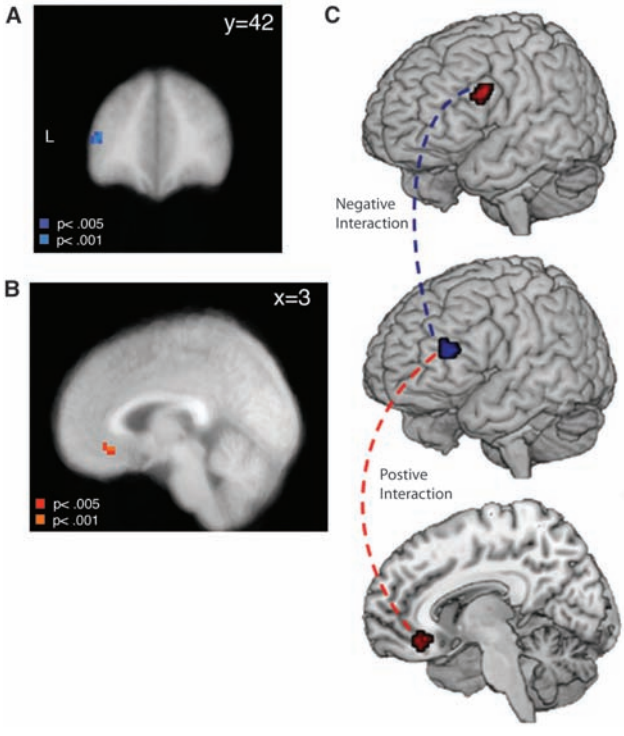

Fig. 4. (**A**) Left IFG/BA46 showed negative task-related functional connectivity with the left DLPFC during decisions about unhealthy items by the SC group. (**B**) Conjunction analysis showing voxels that were correlated with goal values and exhibiting significant positive task-related functional connectivity with IFG/BA46 (reported P values based on the PPI analysis). (**C**) Diagram summarizing the results of the PPI analyses and illustrating the path through which the left DLPFC might modulate activity in the vmPFC. Blue lines represent negative interactions, and red lines represent positive ones. Images and coordinates are in MNI space.

modulate the value signal in order to exercise self-control. Our results bring a substantial amount of resolution to this debate. Like Kable and Glimcher, we find strong evidence for the existence of a common valuation signal in the vmPFC that drives choices regardless of the degree of self-control deployed by the participants. Like McClure *et al*., our results suggest that the DLPFC plays a critical role in the deployment of self-control. Contrary to their theory, however, we show that this is not because an alternative value signal is encoded in DLPFC, which in our experiment would require a nonexistent correlation between activity in this area and the health ratings (fig. S5). Instead, the DLPFC influences self-control by modulating the value signal encoded in vmPFC.

Lastly, an improved understanding of the neurobiology of self-control in decision-making will have applications to clinical practice in domains such as obesity and addiction, to economic and public policy analysis in problems such as suboptimal savings and health behaviors, and to legal thinking about which criteria should be used in determining if an individual is in full command of his decision-making faculties and thus accountable to the law.

References and Notes

1. M. Muraven, D. M. Tice, R. F. Baumeister, *J. Pers. Soc. Psychol.* **74**, 774 (1998).
2. B. Shiv, A. Fedorikhin, *J. Consum. Res.* **26**, 278 (1999).
3. K. D. Vohs *et al*., *J. Pers. Soc. Psychol.* **94**, 883 (2008).
4. G. Ainslie, J. R. Monterosso, *J. Exp. Anal. Behav.* **79**, 37 (2003).
5. W. Mischel, Y. Shoda, M. I. Rodriguez, *Science* **244**, 933 (1989).
6. J. Monterosso, G. Ainslie, *Drug Alcohol Depend.* **90** (suppl. 1), S100 (2007).
7. E. Siegel, H. Rachlin, *J. Exp. Anal. Behav.* **64**, 117 (1995).
8. A. L. Duckworth, M. E. Seligman, *Psychol. Sci.* **16**, 939 (2005).
9. N. A. Shamosh *et al*., *Psychol. Sci.* **19**, 904 (2008).
10. J. P. Tangney, R. F. Baumeister, A. L. Boone, *J. Pers.* **72**, 271 (2004).
11. T. A. Hare, J. O'Doherty, C. F. Camerer, W. Schultz, A. Rangel, *J. Neurosci.* **28**, 5623 (2008).
12. J. W. Kable, P. W. Glimcher, *Nat. Neurosci.* **10**, 1625 (2007).
13. H. Plassmann, J. O'Doherty, A. Rangel, *J. Neurosci.* **27**, 9984 (2007).
14. E. T. Rolls, C. McCabe, J. Redoute, *Cereb. Cortex* **18**, 652 (2008).
15. S. M. Tom, C. R. Fox, C. Trepel, R. A. Poldrack, *Science* **315**, 515 (2007).
16. V. V. Valentin, A. Dickinson, J. P. O'Doherty, *J. Neurosci.* **27**, 4019 (2007).
17. C. Padoa-Schioppa, J. A. Assad, *Nature* **441**, 223 (2006).
18. J. D. Wallis, E. K. Miller, *Eur. J. Neurosci.* **18**, 2069 (2003).
19. C. S. Carter, V. van Veen, *Cogn. Affect. Behav. Neurosci.* **7**, 367 (2007).
20. E. K. Miller, J. D. Cohen, *Annu. Rev. Neurosci.* **24**, 167 (2001).
21. M. Watanabe, K. Hikosaka, M. Sakagami, S. Shirakawa, *Exp. Brain Res.* **166**, 263 (2005).
22. J. Duncan, A. M. Owen, *Trends Neurosci.* **23**, 475 (2000).
23. K. N. Ochsner, J. J. Gross, *Trends Cogn. Sci.* **9**, 242 (2005).
24. Materials and methods are available as supporting material on *Science* Online.
25. D. K. Campbell-Meiklejohn, M. W. Woolrich, R. E. Passingham, R. D. Rogers, *Biol. Psychiatry* **63**, 293 (2008).
26. H. Barbas, D. N. Pandya, *J. Comp. Neurol.* **286**, 353 (1989).
27. D. Badre, A. D. Wagner, *Neuron* **41**, 473 (2004).
28. A. W. MacDonald 3rd, J. D. Cohen, V. A. Stenger, C. S. Carter, *Science* **288**, 1835 (2000).
29. M. R. Delgado, M. M. Gillis, E. A. Phelps, *Nat. Neurosci.* **11**, 880 (2008).
30. S. M. McClure, K. M. Ericson, D. I. Laibson, G. Loewenstein, J. D. Cohen, *J. Neurosci.* **27**, 5796 (2007).
31. S. M. McClure, D. I. Laibson, G. Loewenstein, J. D. Cohen, *Science* **306**, 503 (2004).

32. This work was funded by the Moore Foundation and the Economic Research Service of the U.S. Department of Agriculture on Behavioral Health Economics Research on Dietary Choice and Obesity.

Supporting Online Material

www.sciencemag.org/cgi/content/full/324/5927/646/DC1
Materials and Methods
Figs. S1 to S5
Tables S1 to S5
References

12 November 2008; accepted 12 March 2009
10.1126/science.1168450

Supporting Online Material for

Self-Control in Decision-Making Involves Modulation of the vmPFC Valuation System

Todd A. Hare,* Colin F. Camerer, Antonio Rangel

*To whom correspondence should be addressed. E-mail: thare@hss.caltech.edu

Published 1 May 2009, *Science* **324**, 646 (2009)
DOI: 10.1126/science.1168450

This PDF file includes:

Supporting Online Material

Self-control in Decision-making Involves Modulation of the vmPFC Valuation System

Todd A. Hare
Colin F. Camerer
Antonio Rangel

Materials and Methods

Subjects. Fifty-two subjects participated in the experiment. However 15 subjects did not meet our a priori inclusion criteria based on their behavioral data (see details below). 37 subjects were included in the analysis (20 females, mean age= 25.0 years; age range= 19 – 35 years). Subjects were divided into two groups based on their behavioral data: successful self-controllers (the SC group) and non-self-controllers (the NSC group). The SC group included 19 subjects (14 female, mean age= 26.2 years, age range= 21 – 33 years; mean BMI = 24.8 ± 5.2) and the NSC group included 18 subjects (6 female, mean age= 23.4 years, age range= 19-35 years, mean BMI = 23.2 ± 5.1). All subjects were right-handed, healthy, had normal or corrected-to-normal vision, had no history of psychiatric diagnoses, neurological or metabolic illnesses, and were not taking medications that interfere with the performance of fMRI. Subjects had no history of eating disorders or food allergies to any of the items used in the experiment. Subjects were told that the goal of the experiment was to study food preferences among dieters and gave written consent before participating. We recruited two types of subjects: 1) individuals who self-reported being on a diet to lose or maintain weight, and 2) individuals who self-reported no current monitoring of their diet. All subjects reported that they enjoyed eating sweets, chocolate, and other "junk food" even though they might be restricting them from their current diet. The review board of the California Institute of Technology approved the study.

Stimuli. Subjects rated and made decisions on 50 different food items including junk foods (e.g., chips or candy bars) as well as healthy snacks (e.g. apples or broccoli). The foods were presented to the subjects using high-resolution color pictures (72 dpi). The stimulus presentation and response recording was controlled by E-prime. The visual stimuli were presented using video goggles.

Task. Subjects were instructed not to eat for three hours before the experiment, which is known to increase the value that is placed on food (*1*).

The task had three parts, all of them done in the scanner. Subjects first rated all 50 food items for both their taste and healthiness in two separate blocks (a taste-rating block and a health-rating block). The order of the rating blocks was counterbalanced across subjects and the food items were presented in random order. Ratings were made using a five-point scale that was shown on the screen below each item. The health rating scale was: Very Unhealthy, Unhealthy, Neutral, Healthy, Very Healthy. The taste rating scale was: Very Bad, Bad, Neutral, Good, Very Good.

To preclude responses of no interest in motor areas, the mapping of ratings to button presses was also counterbalanced across subjects. For example, for half of the subjects Very Bad corresponded to a '1' button press and Very Good to a '5' button press, whereas for the other half the opposite order was used. Before the taste-rating block subjects were instructed to "rate the taste of each food item without regard for its healthiness". Before the health-rating block they were instructed to "rate the healthiness of each food item without regard for its taste". Subjects had a maximum of 4 seconds to enter their rating and the trial terminated as soon as they did so. Trials were separated by a random ITI with duration distributed uniformly between 4 and 15 seconds.

Following the two rating blocks, one item that was rated as neutral on both health and taste was selected as the reference food for that subject. Examples of such reference items included wheat crakers, jello, raisins, granola bars, and yogurt. A small number of subjects did not have an item that was rated neutral in both dimensions. In these cases we selected an item that was rated neutral on the taste scale and healthy on the health scale as the reference item. A neutral healthy item was selected because it would still have greater overall value than a liked but unhealthy item for a subject who made decisions based on taste information.

The final session of the experiment was a decision phase. At the beginning of this phase subjects were shown a picture of the reference item and told that on each trial they would have to choose between eating the food item shown in that trial and the reference food. Subjects had a maximum of 4 seconds to enter their decision and the trial terminated as soon as they did so. Trials were separated by a random ITI with duration distributed uniformly between 4 and 15 seconds. Each food item was shown once for a total of 50 trials. Subjects cared about their choices because they were required to eat the food that they chose in a randomly selected trial at the end of the experiment. Note that because subjects did not know which trial would count, their optimal strategy was to treat each decision as if it were the only one that counted. Although this is a binary decision task, subjects were asked to express the strength of their preferences using a five-point scale: Strong No (=choose reference), No (=choose reference item), Neutral, Yes (=choose shown item), Strong Yes (=choose shown item). In the trials in which the subjects choose 'Neutral' a coin was flipped to determine the decision.

Subject classification.

Subjects were classified as self-controllers (SC) or non-self-controllers (NSC) based on their behavior during the experiment, and <u>not</u> on their self-reports about diet status during the recruiting process. In order to be classified as SC, subjects had to meet <u>all</u> of the following three criteria:

1. The subject had to use self-control on more than 50% of the trials in which self-control was required (i.e. decline Liked-Unhealthy items or choose Disliked-Healthy ones). For this analysis, Strong No and No responses were counted as a 'no', and Strong Yes and Yes responses were counted as a 'yes'.
2. In a linear regression model of the decision strength on the health and taste ratings, the coefficient for health had to be greater than the coefficient for taste.

3. The R^2 of a linear regression of the decision strength on the health ratings had to be greater than the R^2 of a linear regression of the decision strength on the taste ratings.

The combination of these three stringent criteria was imposed to make sure that subjects labeled as SCs were exercising self-control in a majority of the experimental trials. Note that subjects in the NSC group used in the data analysis below failed to meet all of the three criteria, and that subjects who met only one or two of the criteria, and thus fell in a gray area between SC and NSC, were excluded from the final analysis.

Note also that there were more females than males in the SC group. To ensure that differences between the SC and NSC groups were not driven by sex differences we conducted the following tests:

1. To test for an effect of sex on the relationship between the effect that health ratings have on vmPFC activity and the effect that the health ratings have on decisions (Fig 2E). We repeated the robust linear regression analysis including sex as an independent variable. The coefficient for sex was not significant ($t = 1.12$) indicating that sex did not influence this relationship. The relationship between the neural beta for health ratings and the behavioral beta for health ratings remained significant ($t = 5.00$, $p < .001$)
2. To test for an effect of sex on BOLD signal in our main regions of interest we conducted three two sample t-tests. There was no difference between males and females in DLPFC activity ($t = -0.38$), taste rating fit to vmPFC activity ($t = 0.48$), or health rating fit to vmPFC activity ($t= -0.54$).

Behavioral data analysis.

Fig. 1B depicts the frequency with which the subjects chose the food item over the reference food in four distinct categories: Disliked-Unhealthy, Disliked-Healthy, Liked-Unhealthy, and Liked-Healthy. Note that the two middle categories require the exercise of self-control, but the first and last do not. There was no difference in mean health ratings ($t = -1.51$, $p = .14$, two-sample t-test) between the SC and NSC groups, indicating that subjects in both groups were equally aware of the health characteristics of the food items. Table S1 lists the reaction time data for both groups.

fMRI data acquisition.

Functional imaging was conducted using a 3.0 Tesla Trio MRI scanner to acquire gradient echo T2*-weighted echoplanar (EPI) images with BOLD contrast. To optimize functional sensitivity in the orbitofrontal cortex (OFC), a key region of interest, we acquired the images in an oblique orientation of 30° to the anterior commissure–posterior commissure line (*2*). In addition, we used an eight-channel phased array coil which yields a 40% increase in signal in the OFC over a standard head coil. Each volume of images had 44 axial slices. A total of 777 volumes were collected over three sessions in an interleaved-ascending manner. The imaging parameters were as follows: echo time, 30 ms; field of view, 192 mm; in-plane resolution and slice thickness, 3

mm; repetition time, 2.75 s. Whole-brain high-resolution T1-weighted structural scans (1 x 1 x 1 mm) were acquired for each subject, coregistered with their mean EPI images, and averaged across subjects to permit anatomical localization of the functional activations at the group level.

fMRI data analysis.

Preprocessing

Image analysis was performed using SPM5 (Wellcome Department of Imaging Neuroscience, Institute of Neurology, London, UK). Images were corrected for slice acquisition time within each volume, motion corrected with realignment to the first volume, spatially normalized to the standard Montreal Neurological Institute EPI template, and spatially smoothed using a Gaussian kernel with a full width at half maximum of 8 mm. Intensity normalization and high-pass temporal filtering (using a filter width of 128 s) were also applied to the data.

General linear models (GLMs)

We used several GLMs with AR(1) to analyze the data.

GLM 1. This model was designed to identify regions in which BOLD activity was parametrically related to goal values, and was estimated on the three parts of the experiment. The model included the following regressors:

1. An indicator function denoting a rating or a decision trial[1];
2. An indicator function denoting a rating or a decision trial multiplied (i.e., modulated) by the subject's goal value for the food item shown in that trial.[2]

Note that both regressors were modeled as box-car functions with a duration equal to the subject's reaction time for that trial. The model also included motion parameters, session constants, and missed trials as regressors of no interest. The regressors of interest and missed trial regressor were convolved with a canonical form of the hemodynamic response.

Note that this GLM makes use of parametric regressors. These types of regressors are used to look for areas in which the BOLD response varies with the magnitude of a variable of interest (in this case the goal value). The estimated coefficient for such regressors can be roughly interpreted as a measure of the strength of the association between the BOLD response and the variable of interest.

[1] The indicator function equals 1 whenever the event occurred, and equals 0 otherwise.

[2] The goal value for each item was measured by the decision strength (strong no – strong yes). Although decisions were only made during the decision block, the goal value measures were transferred to the corresponding food items in the health and taste rating blocks to create the regressor for all blocks.

Single subject contrasts were calculated for the difference between the parametric regressor for goal value in the decision block and the parametric regressor for goal value in the taste-rating block. This contrast was motivated by previous work by Plassmann et. al. (*3*) and it identifies regions where BOLD activity is more correlated with the goal values in choice trials, when a goal value needs to be computed by the brain, than in rating trials, in which some aspect of the item was evaluated without having to make a decision.

We then estimated a second-level mixed effects analysis over all of the subjects (both SC and NSC) by computing one-sample *t* tests on the single-subject contrast coefficients. The results are shown in Fig. 2A and reported in Table S2. For visualization purposes only, all of the images shown in the paper and supplementary materials are thresholded at $p < .001$ and $p < .005$ uncorrected. For inference purposes, the areas reported in Table S2 are whole brain corrected at the cluster level based on the algorithm implemented in the CorrClusTh program by Thomas Nichols (http://www.sph.umich.edu/~nichols/JohnsGems5.html). All anatomical localizations were performed by overlapping the *t*-maps on a normalized structural image averaged across subjects, and with reference to an anatomical Atlas (*4*).

Fig. S1 shows the average beta values (i.e., the estimated coefficients) for goal value within the vmPFC region of interest (ROI) shown in Fig. 2A for the SC and NSC groups separately. Beta values were extracted from individual subject peaks within this ROI to allow for variability between subjects. The mean and standard error of these betas were computed for each group.

GLM 2. In order to explore further the results depicted above, we estimated an additional post-hoc GLM using the data from the decision session only. This model included the following five regressors:

1. An indicator function denoting a 'Strong-No' trial;
2. An indicator function denoting a 'No' trial;
3. An indicator function denoting a 'Neutral' trial;
4. An indicator function denoting a 'Yes' trial;
5. An indicator function denoting a 'Strong-Yes' trial;

Note that all of the regressors were modeled as box-car functions with a duration equal to the subject's reaction time for that trial. The model also included motion parameters and missed trials as regressors of no interest. The regressors of interest and the missed trials regressor were convolved with a canonical form of the hemodynamic response.

Fig. 2B shows the estimated betas in the vmPFC for each of the regressors. This plot was constructed as follows. First, for each individual and type of trial we measured the associated beta value at the peak voxel for the goal value contrast (GLM 1) inside the vmPFC ROI shown in Fig. 2A. The individual subject peaks were selected from within this ROI to allow for variability between subjects. Second, the mean and standard error of these betas were computed for each type of trial.

GLM 3. An additional GLM was estimated to explore the extent to which taste and health considerations were reflected in the activity of the vmPFC. The model was estimated in the three parts of the experiment. It included the following regressors:

1. An indicator function denoting a rating or a decision trial;
2. An indicator function denoting a rating or a decision trial multiplied by the subject's health rating;
3. An indicator function denoting a rating or a decision trial multiplied by the subject's taste rating.

Note that subjects' health and taste ratings were not correlated (SC group mean r = 0.033; NSC group mean r = -0.040). All of the regressors were modeled as box-car functions with a duration equal to the subject's reaction time for that trial. The model also included motion parameters, session constants, and missed trials as regressors of no interest. The regressors of interest and missed trial regressor were convolved with a canonical form of the hemodynamic response.

Fig. 2D shows the average beta values for the parametric regressors for health and taste in the SC and NSC groups in the vmPFC. To maximize the comparability of the results, the beta values were extracted from the same individual subject peaks used in Fig. 2B.

GLM 4. This model was designed to identify regions whose activity increased during successful self-control. Self-control can only be exercised during the act of choosing, and therefore, the model was estimated only on the decision block. It included the following regressors:

1. An indicator function denoting a trial in which self-control was required (i.e. Healthy-Disliked and Unhealthy-Liked trials) and successfully deployed.
2. An indicator function denoting a trial in which no self-control was required (i.e. Unhealthy-Disliked and Healthy-Liked trials);
3. An indicator function denoting a trial in which self-control was required but not deployed.
4. An indicator function denoting a trial in which the subject selected the "neutral" response and therefore did not make a decision.

Note that all of the regressors were modeled as box-car functions with a duration equal to the subject's reaction time for that trial. The model also included motion parameters and missed trials as regressors of no interest. The regressors of interest and missed trial regressor were convolved with a canonical form of the hemodynamic response.

The following contrasts were computed for each subject: (1) successful self-control, (2) failed self-control, and (3) the difference between successful and failed self-control trials.

We then estimated a second-level contrast by performing a two-sample *t* test on successful self-control trials between the SC and the NSC groups (three subjects from the NSC group were excluded from this contrast because they never used self-control). The results are shown in Fig. 3A and reported in Table S3. The areas reported in Table S3 are small volume corrected at the cluster level (cluster size 21 voxels, Z = 2.74). The small volume correction was based on a

bilateral mask of the voxels in DLPFC that were active in the SC group for successful self-control trials versus baseline at $p < .05$ after FWE correction.

Fig. 3B shows the beta values for successful self-control trials and failed self-control trials for both groups. The beta values were extracted from the individual subject peaks for the contrast successful minus failed self-control within the ROI in Fig. 3A. Four subjects from the SC group were excluded from this analysis because they always used self-control, and three subjects from the NSC group were excluded from this contrast because they never used self-control.

Psychophysiological interactions (PPIs)

We also estimated the following PPI models.

PPI 1. The goal of this analysis was to investigate if activity in the left DLPFC (IFG/BA 9) was correlated with activity in the vmPFC during decision trials requiring self-control.

The analyses proceed in three steps.

First, we computed individual average time-series within a 4mm sphere surrounding individual subject peaks within the functional mask of left IFG/BA 9 shown in Fig. 3A. Variance associated with the six motion regressors was removed from the extracted time-series. The location of the peak voxels was based on a post-hoc GLM was that computed for the sole purposes of this PPI analysis. This GLM was estimated on the decision block and included two separate regressors: one for trials where a healthy food was shown, and one for trials in which an unhealthy food was presented.[3] Individual subject peaks within the left IFG/BA9 mask were then identified based on the areas having the strongest positive response in unhealthy trials. The seed time-courses were then deconvolved, based on the formula for the canonical hemodynamic response, in order to construct a time series of neural activity in left IFG/BA9. This was done following the procedures described in Gitelman et al. (*5*).

Second, we estimated a GLM with the following regressors in the decision block only:

1. An interaction between the neural activity in the seed region and an indicator function for unhealthy trials;
2. An indicator function for unhealthy trials;
3. The original BOLD eigenvariate. (i.e. the average time-series from the 4mm sphere)

The first two regressors were convolved with a canonical form of the hemodynamic response. The model also included motion parameters as regressors of no interest.

[3] This model was used in place of GLM 4 in order to increase the number of trials used in the analysis and the variability of activity in the seed region. Note that self-control is mostly exercised by the SC group during trials with Unhealthy-Liked items.

Note that the first regressor identifies areas that exhibit task-related functional connectivity with IFG/BA9. In particular, it identifies areas in which the correlation in BOLD activity with IFG/BA9 increases during unhealthy trials.

Third, single subject contrasts for the first regressor were calculated, and then a second level analysis was performed by calculating a one-sample *t* test on the single-subject contrast coefficients. The results of the second level contrast at $p < .005$ uncorrected and a 15 voxel extent threshold are depicted in Fig. 4A and Table S4.

As shown in Table S4, this first PPI analysis identified multiple regions in which activity correlated with left IFG/BA 9 during the trials in which subjects made decisions about unhealthy foods. We chose an area of left IFG/BA 46 as a seed for a further PPI analysis. This area was selected for the reasons mentioned in the text. Additionally, a post-hoc two-sample t-test showed that there was stronger task related connectivity between the left IFG/BA9 and IFG/BA46 areas in the SC than in the NSC group ($t = 2.88$, $p < .01$, Fig. S4). This t-test was based on the average beta value across all voxels in the IFG/BA 46 region at $p < .005$.

PPI 2. We carried out a PPI analysis using the left IFG/BA 46 as a seed. This PPI analysis was identical to the previous one, except that the average time-series used in the first step of the analysis were extracted from individual subject peaks within the functional ROI in the left IFG/BA 46 identified by the first PPI analysis at a threshold of $p < .005$ uncorrected. Individual subject peaks were identified based on the strength of correlation between activity isn the left IFG/BA46 and the left IFG/BA9. The results are described in Table S5.

To further investigate the results of this PPI analysis, we carried out a conjunction analysis by finding the intersection of voxels that were significant in contrast for goal value at $p < .05$ whole brain cluster corrected and that also exhibited significant task related functional connectivity with left IFG/BA 46 at $p < .005$ uncorrected with an extent threshold of 15 voxels. The results are depicted in Table S5 and Fig. 4B.

Note that the regions illustrated from top to bottom in Fig 4C. are 3D projections of the functional ROIs shown in Figs 3A, 4A, and 4B, respectively.

Post-hoc robust regressions

We performed two post-hoc robust linear regressions to explore the results further.

First, we regressed a behavioral measure of the influence that health considerations had on decisions on a neural measure of the impact that health ratings had on vmPFC activity. Each subject was an observation. The behavioral measure was given by the estimated coefficient for health in a regression of health and taste ratings on decision strength (goal value). The neural measure was the beta value for health rating at the individual subject peaks in vmPFC as described in the procedures for Fig. 2B. The results of this analysis are depicted in Fig. 2E.

Second, we regressed a neural measure for activity in left IFG/BA 9 on a measure of neural activity in vmPFC during decision trials for liked-unhealthy items. Each subject was an

observation. The independent variable was the beta value for successful self-control trials at individual peak voxels from the left IFG/BA 9 ROI in Fig. 3B. The dependent variable was estimated using a post-hoc GLM were decision trials were spilt into four regressors based on the health and taste ratings (Disliked-Unhealthy, Disliked-Healthy, Liked-Unhealthy, Liked-Healthy). The dependent variable was given by the beta value for each subject for the liked-unhealthy regressor extracted at individual peak voxels from a vmPFC ROI.

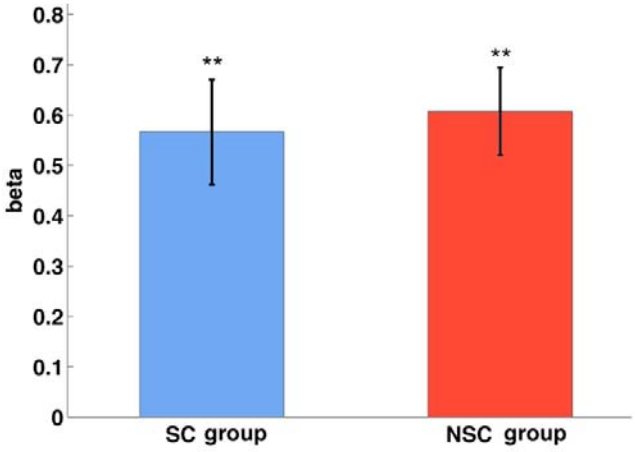

Fig. S1. Average betas representing the correlation between vmPFC activity and goal values in both groups. The blue bar shows the mean ± standard error for the SC group ($t_{18} = 5.44$, $p < .0001$) and the red bar shows the mean ± standard error for the NSC group ($t_{17} = 6.96$, $p < .0001$).

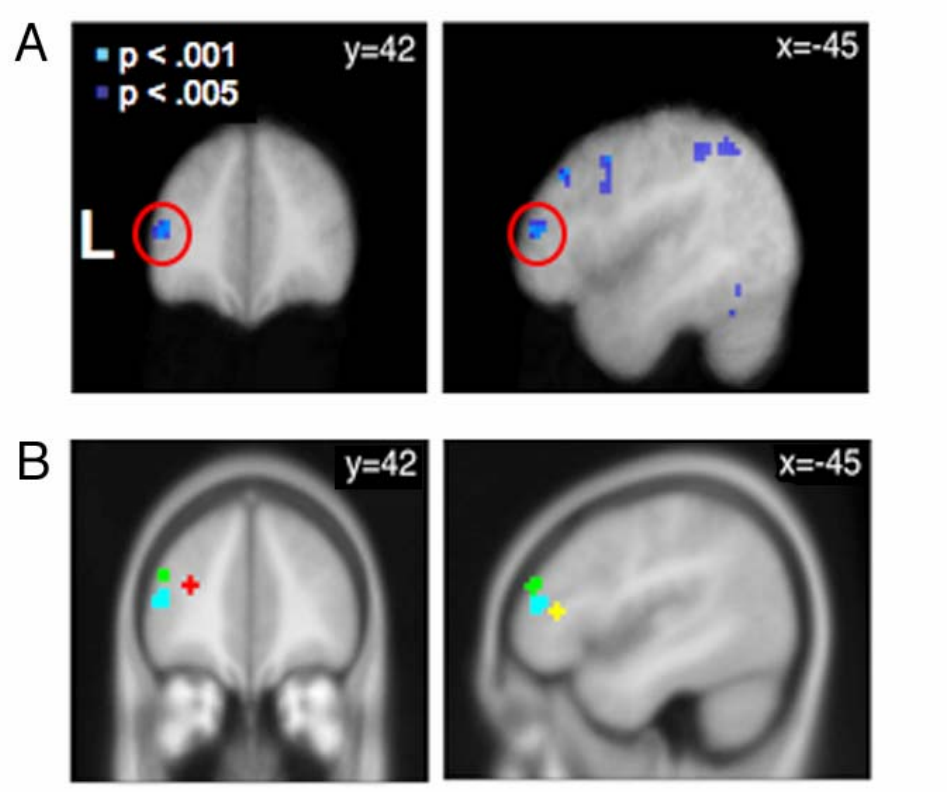

Fig. S2. A) Statistical parametric map displaying all regions showing negative task related functional connectivity with IFG/BA 9 in the SC group at $p < .005$ and an extent threshold of 15 voxels. The IFG/BA 46 region is circled in red. B) Areas of IFG in which activity has been shown to correlate with goal values in previous studies. Light blue: the area of IFG/BA 46 from part (A). Green: taken from Plassmann et. al. (*3*). Yellow: taken from Hare et. al. (*6*). Red: area correlating with goal values ($p < .005$ unc.) in the current study for a contrast that includes all subjects. Note that for ease of comparability the sign of the x-coordinates has been inverted for the areas reported in (*3*, *6*) so that they show up on the left side (in the original papers the peaks of activation occurred in the right IFG).

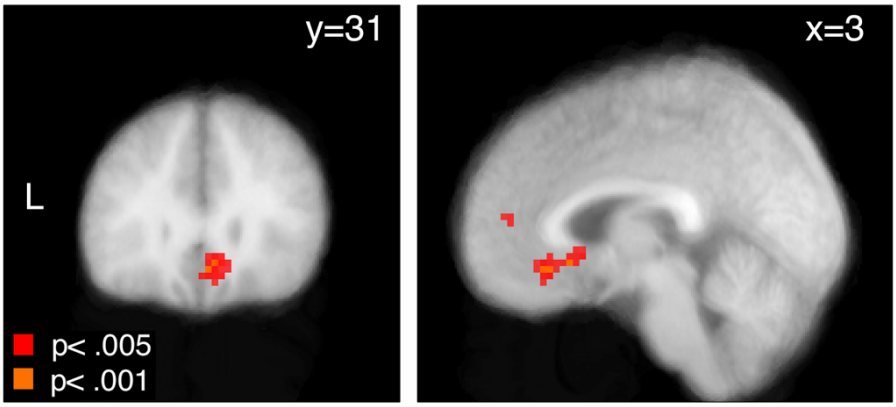

Fig. S3. Statistical parametric map of voxels in the vmPFC showing task related functional connectivity (PPI) with IFG/BA 46 in the SC group.

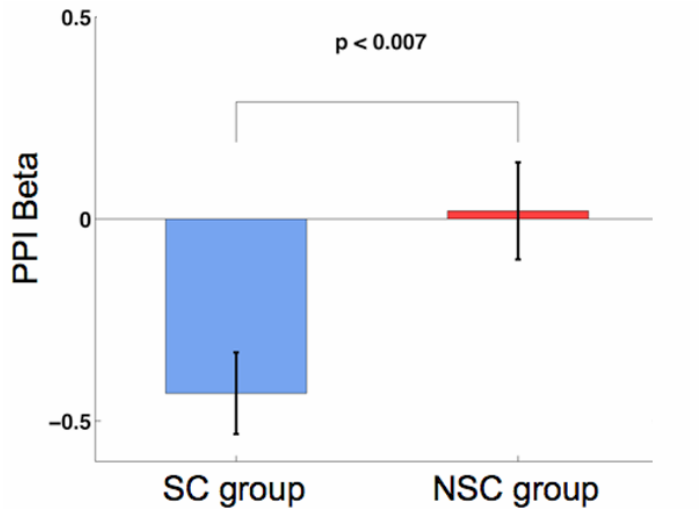

Fig. S4. Average beta values measuring the correlation between BOLD activity in IFG/BA9 and IFG/BA46 in the SC and NSC groups ($t = 2.88$, $p < .007$). The blue bar shows the mean ± standard error for the SC group. The red bar shows the mean ± standard error for the NSC group.

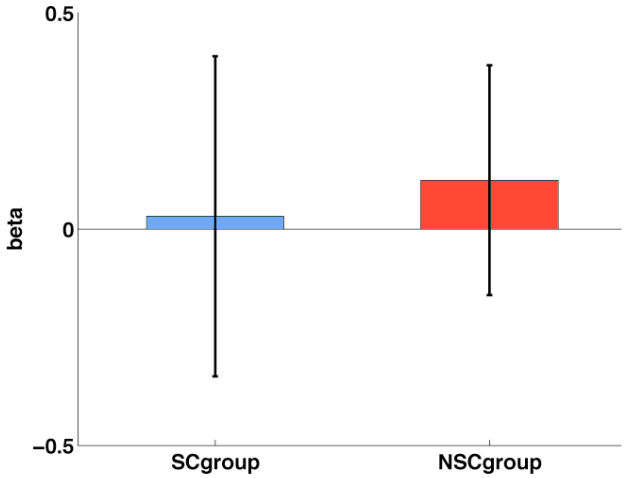

Fig. S5. Effect sizes for the parametric regressor for health ratings from GLM 3 in IFG/BA 9. The blue bar shows the mean and confidence interval for the SC group. The red bar shows the mean and confidence interval for the NSC group. Average beta values were extracted from all voxels within the IFG/BA 9 ROI shown in Fig. 3A at $p < .005$ uncorrected.

Table S1. Mean reaction times by rating and self-control status.

Food Rating	*SC group*	*NSC Group*
Disliked-Unhealthy	1390 (SEM=77)	1882 (SEM=183)
Disliked-Healthy	2175 (SEM=173)	1651 (SEM=197)
Liked-Unhealthy	1710 (SEM=83)	1708 (SEM=103)
Liked-Healthy	1591 (SEM=102)	1732 (SEM=119)

Values are in milliseconds.

Table S2. GLM 1. Areas exhibiting a stronger correlation with goal values during decision trials than during taste-rating trials.

Region	*Side*	*BA*	*MNI Coordinates*	*Z*
Anterior Cingulate /Medial Frontal Gyrus	R	10/32	3 51 3	3.54*
Anterior Cingulate /Medial Frontal Gyrus	L	10/32	-3 45 6	3.34*
Medial Orbital Frontal Cortex	R	11	3 36 -12	2.99*
Middle Frontal Gyrus	L	9/10	-30 42 18	3.1
Anterior Cingulate	L	32	-3 39 21	2.95

*significant at $p < .05$ after whole brain cluster correction with a *t* threshold of 2.72 and an extent of 156 voxels (4212 mm^3)

For completeness, peaks are reported for all clusters $\geq$ 25 voxels at $p < .005$ unc.

Table S3.GLM 4. Areas exhibiting a stronger response in successful self-control trials in the SC group than in the NSC group.

Region	*Side*	*BA*	*MNI Coordinates*	*Z*
Inferior Frontal Gyrus	L	9	-48 15 24	3.63*
Precentral Gyrus	R	4	27 -27 66	4.04
Inferior Parietal/Superior Temporal Gyrus	R	40/42	60 -36 18	3.87
Precentral Gyrus	L	4	-48 -12 48	3.84
Medial Frontal/Cingulate Gyrus	R	6/24	12 -18 42	3.7
Inferior Parietal/Superior Temporal Gyrus	L	40/42	-60 -33 21	3.69
Putamen	L		-21 -3 -3	3.3
Precuneus	L	5	-12 -42 60	3.29
Precentral Gyrus	L	6	-21 -21 66	3.27
Putamen	R		18 0 0	3.21
Precentral Gyrus	R	4/6	42 -12 45	3.06

*significant at $p < .05$ after on small volume correction at the cluster level with a *t* threshold of 2.72 and an extent of 21 voxels (567 mm^3). Small volume correction was based on a bilateral functional mask of voxels in DLPFC that were active in the SC group for successful self-control trials versus baseline at $p < .05$ after FWE correction.
For completeness, peaks are reported for all clusters ≥ 25 voxels at $p < .005$.

Table S4. PPI 1. Regions showing task related functional connectivity with the left IFG/BA9.

Region	*Side*	*BA*	*MNI Coordinates*	*Z*
Positive				
Medial Frontal Gyrus	R	10	12 51 3	2.91
Negative				
Inferior and Superior Parietal Lobule	L	7/40	-27 -60 51	4.1
Middle Frontal Gyrus	R	9	54 30 30	3.94
Cerebellum-Culmen	R		42 -48 -30	3.78
Lingual Gyrus	R	18	9 -90 -3	3.75
Inferior Frontal Gyrus†	L	46	-45 42 12	3.74
Cerebellum-Vermis	L		-3 -42 -15	3.69
Fusiform Gyrus	L	37	-42 -51 -24	3.66
Cerebellum-Vermis	R		3 -54 -33	3.59
Cerebellum-Declive	R		9 -84 -24	3.57
Parahippocampal Gyrus/Midbrain	L		-12 -27 -15	3.51
Fusiform Gyrus	R	19	33 -78 -21	3.48
Medial Frontal Gyrus	L	8	-3 24 45	3.43
Inferior and Superior Parietal Lobule	R	7/40	33 -66 45	3.39
Middle Frontal Gyrus	R	9	-54 15 36	3.36
Middle Occipital Gyrus	R	17	-9 -96 -3	3.28
Cuneus	R	30	-9 -63 6	3.17
Cingulate Gyrus	R	23	-3 -27 33	3.01
Middle Occipital Gyrus	L	37	-48 -69 -6	2.98

Threshold: 15 voxels, $p < .005$ uncorrected.
† seed region for PPI analysis reported in Table S5.

Table S5. PPI 2. Regions showing positive task related functional connectivity with the left IFG/BA46 region.

Region	*Side*	*BA*	*MNI Coordinates*	*Z*
Medial Orbitofrontal Cortex	R	11	3 33 -12	3.25*
Anterior Cingulate/Medial Frontal Gyrus	L	10/32	-3 48 12	3.04
Medial Frontal Gyrus	R	10	12 51 0	3.01

Threshold: 15 voxels, $p < .005$ uncorrected.

* peak for conjunction analysis of all voxels showing 1) significant task related functional connectivity with the left IFG/BA46 at $p<.005$ uncorrected and 2) a significant correlation with goal value at $p<.05$ whole brain cluster corrected.

References

1. E. L. Gibson, E. Desmond, *Appetite* **32**, 219 (1999).
2. R. Deichmann, J. A. Gottfried, C. Hutton, R. Turner, *NeuroImage* **19**, 430 (2003).
3. H. Plassmann, J. O'Doherty, A. Rangel, *J Neurosci* **27**, 9984 (2007).
4. H. M. Duvernoy, *The Human Brain: Surface, Three-Dimensional Sectional Anatomy with MRI, and Blood Supply* (Springer, Berlin, 1999), pp.
5. D. R. Gitelman, W. D. Penny, J. Ashburner, K. J. Friston, *NeuroImage* **19**, 200 (2003).
6. T. A. Hare, J. O'Doherty, C. F. Camerer, W. Schultz, A. Rangel, *J Neurosci* **28**, 5623 (2008).